Quadrature Histograms in Maximum Likelihood Quantum State Tomography

J. L. E. Silva,[1] H. M. Vasconcelos,[1, 2, *] and S. Glancy[2]

[1] *Departamento de Engenharia de Teleinformática, Universidade Federal do Ceará, Fortaleza, Ceará, 60440, Brazil*

[2] *Applied and Computational Mathematics Division, National Institute of Standards and Technology, Boulder, Colorado, 80305, USA*

(Dated: March 15, 2018)

Quantum state tomography aims to determine the quantum state of a system from measured data and is an essential tool for quantum information. When dealing with continuous variable quantum states of light, QST is often done by measuring the field amplitudes at different optical phases using homodyne detection. The quadrature-phase homodyne measurement outputs a continuous variable, so to reduce the computational cost of tomography, researchers often discretize the measurements into histogram bin. We show that this can be done without significantly degrading the fidelity of the estimated state. This paper tests different strategies for determining the histogram bins.

PACS numbers: 03.65.Wj, 03.67.-a, 42.50.Dv

I. INTRODUCTION

Quantum information science and engineering are at the point where rudimentary quantum computers are available in the laboratory and commercially [1–4]. However, further advancing quantum technologies requires improvements in the fidelities of basic operations. Consequently, more precise and efficient reconstruction and diagnostic tools used to estimate quantum states [5–12], processes [13–20], and measurements [21–24] are essential.

Quantum tomography techniques for optical quantum states of light has become a standard tool because quantum light sources are essential for implementations of continuous-variable (CV) quantum computation [25–29]. These source are also extensively exploited in quantum criptography [30–34], quantum metrology [35, 36], state teleportation [37–39], dense coding [40, 41] and cloning [42, 43].

In quantum state tomography, we perform a measurement on each member of a collection of quantum systems, prepared in the same unknown state. The goal is to estimate this unknown state from the measurements results. This estimation can be done by different methods, but we study Maximum Likelihood Estimation (MLE), which finds among all possible states, the one that maximizes the probability of obtaining the observed data.

Quantum homodyne tomography is one of the most popular optical tomography techniques available [44]. It rapidly became a versatile tool and has been applied in many different quantum optics experimental settings since it was proposed by Vogel and Risken in 1989 [5] and first implemented by Smithey *et al.* in 1993 [6]. This technique permits one to characterize an optical quantum state by analyzing multiple phase-sensitive measurements of the field quadratures.

A homodyne measurement generates a continuous value. Although discretization is not absolutely necessary, it is a popular practice, and we believe that the information lost by discretization may be insignificant. On the other hand, discretization of the data considerably reduces the size of the data, expediting the reconstruction algorithm. How should we choose a discretization strategy such that the bins are not too small nor too big? Larger bins will reduce calculation time and memory, but bins should not be too large in order to avoid a lack of resolution, making the histogram a poor representation of the underlying distribution.

In this paper, we use numerical experiments to simulate optical homodyne tomography and perform maximum likelihood tomography on the data with and without discretization. When choosing a quadrature bin width, we use and compare two different strategies: Scott's rule [45] and Leonhardt's formula [46]. The paper is divide as follow: we begin by reviewing maximum likelihood in homodyne tomography in Section II. Then, in Section III, we describe our numerical experiments. Next, we discuss the estimation of the mean photon number from the quadrature measurements in Section IV. In Section V we present our results, and we make our concluding remarks in Section VI.

II. MAXIMUM LIKELIHOOD IN HOMODYNE TOMOGRAPHY

Let us consider N quantum systems, each prepared in an optical state described by a density matrix ρ_{true}. In each experimental trial i, we measure the field quadrature of one of the systems at some phase θ_i of a local oscillator, i.e. a reference system prepared in a high amplitude coherent state. Each measurement is associated with an observable $\hat{X}_{\theta_i} = \hat{X}\cos\theta_i + \hat{P}\sin\theta_i$, where $\hat{X}$ and $\hat{P}$ are analogous to mechanical position and momentum operators, respectively. For a given phase θ_i, we measure a quadrature value x_i, resulting in the data set

* hilma@ufc.br

$\{(\theta_i, x_i)|i = 1, \ldots, N\}$.

The outcome of the i-th measurement is associated with a positive-operator-valued measure (POVM) element $\Pi(x_i|\theta_i) = \Pi_i$. Given the data set, the likelihood of a candidate density matrix ρ is

$$\mathcal{L}(\rho) = \prod_{i=1}^{N} \mathrm{Tr}(\Pi_i \rho), \tag{1}$$

where $\mathrm{Tr}(\rho\Pi_i)$ is the probability, when measuring with phase θ_i, to obtain outcome x_i, according to the candidate density matrix ρ.

MLE searches for the density matrix that maximizes the likelihood in (1). Equivalently, it usually is more convenient to maximize the logarithm of the likelihood (the "log-likelihood"):

$$L(\rho) = \ln \mathcal{L}(\rho) = \sum_{i=1}^{N} \ln[\mathrm{Tr}(\Pi_i \rho)], \tag{2}$$

which is maximized by the same density matrix as the likelihood. The MLE is essentially a function optimization problem, and since the log-likelihood function is concave, convergence to a unique solution will be achieved by most iterative optimization methods.

In our numerical simulations, we use an algorithm for likelihood maximization that begins with iterations of the $R\rho R$ algorithm [47] followed by iterations of a regularized gradient ascent algorithm (RGA). The main reason to switch from one algorithm to another is that a slow-down is observed in the $R\rho R$ algorithm after about $(n+1)^2/4$ iterations. In the RGA, $\rho^{(k+1)}$ is parametrized as

$$\rho^{(k+1)} = \frac{\left(\sqrt{\rho^{(k)}} + A\right)\left(\sqrt{\rho^{(k)}} + A^\dagger\right)}{\mathrm{Tr}\left[\left(\sqrt{\rho^{(k)}} + A\right)\left(\sqrt{\rho^{(k)}} + A^\dagger\right)\right]}, \tag{3}$$

where $\rho^{(k)}$ is the density matrix found by the previous iteration, and A may be any complex matrix of the same dimensions as ρ. Eq. (3) ensures that $\rho^{(k+1)}$ is a density matrix for any A. The matrix A is chosen to maximize the quadratic approximation of the log-likelihood subject to $\mathrm{Tr}(AA^\dagger) \leq u$, where u is a positive number adjusted by the algorithm to guarantee that the log-likelihood increases with each iteration. To halt the iterations, we use the stopping criterion of [48], $L(\rho_{\mathrm{ML}}) - L(\rho^{(k)}) \leq 0.2$, where $L(\rho_{\mathrm{ML}})$ is the maximum of the log-likelihood.

III. NUMERICAL EXPERIMENTS

Our numerical experiments simulate single mode optical homodyne measurements of two types of states: (1) superpositions of coherent states of opposite phase $|-\alpha\rangle + |\alpha\rangle$ (called "cat states") and (2) squeezed vacuum states. Each state is represented by a density matrix ρ_{true} truncated in a n photon basis.

In order to calculate the probability to obtain homodyne measurement outcome x, when measuring state ρ_{true} with phase θ, we need to represent $\Pi(x|\theta)$ in the n photon basis. If $|x\rangle$ is the photon number basis representation of the x-quadrature eigenstate with eigenvalue x, and $U(\theta)$ is the phase evolution unitary operator, then for an ideal homodyne measurement, we have $\Pi(x|\theta) = U(\theta)^\dagger|x\rangle\langle x|U(\theta)$. To include photon loss or detector inefficiency, we replace the projector with $\Pi(x|\theta) = \sum_{i=1}^{n} E_i(\eta)^\dagger U(\theta)^\dagger|x\rangle\langle x|U(\theta)E_i(\eta)$, where η is the detection efficiency [44]. Typical state-of-the-art homodyne detection systems have efficiency $\eta \sim 0.9$, so we use this value in our simulations. Using this strategy, we are able to correct for the loss as we estimate the state. We use rejection sampling from the distribution given by $P(x|\theta)$ to guarantee random samples of homodyne measurement results [49].

To choose the phases at which the homodyne measurements are performed, we divide the upper-half-circle evenly among m phases between 0 and π and measure N/m times at each phase, where N is the total number of measurements. In all simulations, we use $m = 20$ and $N = 20,000$. To secure a single maximum of the likelihood function, we need an informationally complete set of measurement operators, which can be obtained if we use $n+1$ different phases to reconstruct a state that contains at most n photons [50].

To quantify the similarity of the reconstructed state ρ to the true state ρ_{true} we use the fidelity

$$F = Tr\sqrt{\rho^{1/2}\,\rho_{\mathrm{true}}\,\rho^{1/2}}. \tag{4}$$

We report fidelities for four different situations: (i) the state is reconstructed using the continuous values of homodyne measurement results, that is without discretization; (ii) the state is reconstructed with chosen bin widths (iii) the state is reconstructed with bin widths given by Scott's rule [45]; and (iv) the state is reconstructed with bin widths suggested by Leonhardt in [50]. We only consider histograms with contiguous bins of equal width for each phase.

In 1979 Scott derived a formula recommending a bin width for discretizing data sampled from a probability density function f for a single random variable x. The recommended bin width is

$$h^\star = \left[\frac{6}{s\int_{-\infty}^{\infty} f'(x)^2 dx}\right]^{1/3}, \tag{5}$$

where the first and second derivatives of f must be continuous and bounded and s is the sample size. Because one does not know f in an experiment we assume a normal distribution. For a normal f we have

$$\int_{-\infty}^{\infty} f'(x)^2 dx = \frac{1}{4\sqrt{\pi}\sigma^3}, \tag{6}$$

where σ is the distribution's standard deviation. Combining Eqs. (5) and (6), we obtain the recommended bin width for a normal distribution:

$$h = 3.5\,\sigma\,s^{-1/3}. \tag{7}$$

This formula is known as Scott's rule, and is optimal for each phase if the data is normally distributed. In our simulations we compute a bin size separately for each phase's quadrature measurements, and we use the corrected sample standard deviation in place of σ.

Although Scott's rule is optimal for each phase, it may not be optimal for homodyne tomography because we are estimating the density matrix rather than each phase's quadrature distribution individually. Also many interesting optical states do not have normal quadrature distributions, for example our cat states. In fact, one might expect that the bin width should be related to the number of photons in a quantum state because higher photon number states have more narrow features in their quadrature distributions, which should not be washed-out by the discretization.

Leonhardt states that if we desire to reconstructed a density matrix of a state with n photons, we need a bin width narrower than $q_n/2$, where q_n is given by

$$q_n = \frac{\pi}{\sqrt{2n+1}}. \tag{8}$$

This result was obtained by using a semiclassical approximation for the amplitude pattern functions in quantum state sampling [46]. Leonhardt recommends using the maximum photon number in Eq. (8), however many states have no maximum photon number, and whether a state has a true maximum photon number is not possible to learn with certainty from tomography. Instead, we have tested using the photon number at which the reconstruction Hilbert space is truncated M and an estimate of the mean photon number $\overline{\langle \hat{n} \rangle}$ in Eq. (8). The truncation must be chosen in advance to be large enough that the probability that ρ_{true} contains more photons than the truncation limit is very small. We estimate the mean photon number from the quadrature measurements as described in the next section.

IV. ESTIMATING MEAN PHOTON NUMBER

In order to use Leonhardt's advice for choosing the histogram bin width, we need to estimate the mean number $\langle n \rangle$ of photons in the measured state from the phase-quadrature data set. To find an estimator, we first compute the mean value of $(\hat{X}_\theta)^2$, averaged over θ, treating θ as if it is random and uniformly distributed between 0 and π.

$$\langle (\hat{X}_\theta)^2 \rangle = \langle \hat{X}^2 \cos^2\theta + (\hat{X}\hat{P} + \hat{P}\hat{X})\cos\theta\sin\theta + \hat{P}^2\sin^2\theta \rangle \tag{9}$$

The phase θ is independent of $\hat{X}$ and $\hat{P}$, so we can compute the expectation over θ as

$$\begin{aligned} \langle (\hat{X}_\theta)^2 \rangle &= \Big\langle \int_0^\pi (\hat{X}^2\cos^2\theta + (\hat{X}\hat{P} + \hat{P}\hat{X})\cos\theta\sin\theta \\ &\qquad + \hat{P}^2\sin^2\theta)\text{Prob}(\theta)\mathrm{d}\theta \Big\rangle \quad (10) \\ \langle (\hat{X}_\theta)^2 \rangle &= \Big\langle \int_0^\pi (\hat{X}^2\cos^2\theta + (\hat{X}\hat{P} + \hat{P}\hat{X})\cos\theta\sin\theta \\ &\qquad + \hat{P}^2\sin^2\theta)\frac{1}{\pi}\mathrm{d}\theta \Big\rangle \quad (11) \\ &= \frac{1}{2}\left\langle \hat{X}^2 + \hat{P}^2 \right\rangle. \quad (12) \end{aligned}$$

Because the photon number operator is

$$\hat{n} = \frac{1}{2}\left(\hat{X}^2 + \hat{P}^2 - 1\right), \tag{13}$$

we obtain

$$\langle \hat{n} \rangle = \langle \hat{X}_\theta^2 \rangle - \frac{1}{2}. \tag{14}$$

We estimate $\langle \hat{n} \rangle$ by computing the sample mean of all quadrature measurements [51, 52]:

$$\overline{\langle \hat{n} \rangle} = \frac{1}{N}\sum_{i=1}^{N} x_i^2 - \frac{1}{2}. \tag{15}$$

Note that when θ is uniformly distributed over $[0, \pi)$, the values of θ are not needed to compute $\overline{\langle \hat{n} \rangle}$.

V. RESULTS

In our study, we compute the fidelities between the true state and (i) the density matrix reconstructed without discretization, ρ_{ML2}; (ii) the density matrix reconstructed using histograms with chosen bin widths, ρ_{Hist}; (iii) and the density matrix reconstructed using histograms with a bin width given by Scott's method, ρ_{Scott}.

To make the graphs below, for each choice of parameters, we simulate 100 tomography experiments, making 100 density matrix estimates. The graphs show the arithmetic mean of the 100 fidelities of the reconstructed states. The error bars show the standard deviation of the 100 fidelities.

Our first result is shown in Fig. 1. The state considered is a cat state with $\alpha = 1$, where α is the amplitude of the coherent state in the superposition. The state is reconstructed in a Hilbert space truncated at $M = 10$ photons. Scott's method finds a different optimal bin width for each phase considered, so we report the mean bin width averaged over the 20 phases in these cases. Here the mean bin width for Scott's method is 0.35. When choosing a bin width, we go up to 0.34, the value we obtain when we use Eq. (8) for $M = 10$, the number of photons at which we truncated the Hilbert space. In all cases, each bin's

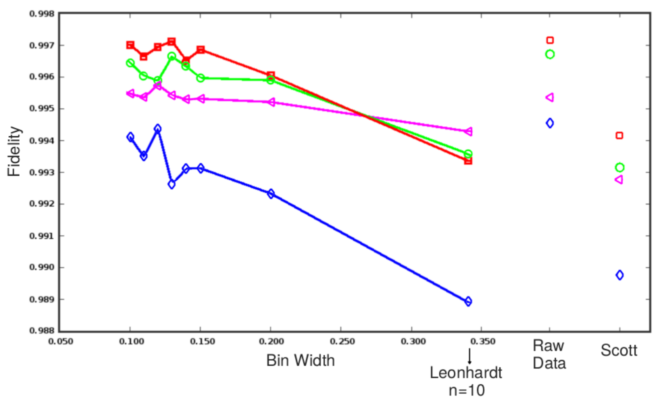

FIG. 1. Average fidelity as a function of the bin width for a cat state with amplitude $\alpha = 1$. The Hilbert space is truncated at $M = 10$ photons. Each set of points with the same color and marker shape corrresponds to a different data set. The mean bin width for Scott method is 0.35.

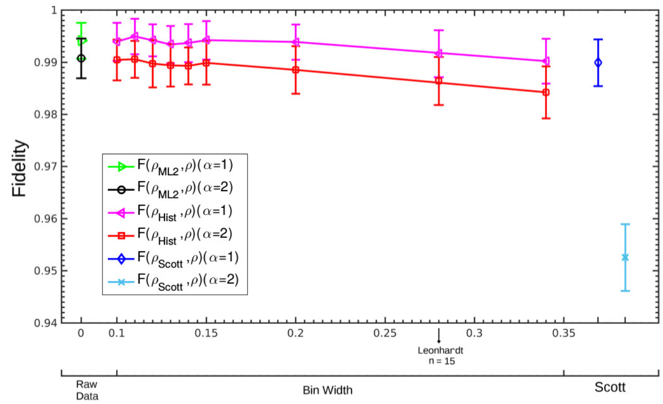

FIG. 2. Average fidelity as a function of the bin width for cat states with amplitudes $\alpha = 1$ and $\alpha = 2$. The Hilbert space is truncated at $M = 15$ photons. The mean bin width for Scott's method are 0.35 ($\alpha = 1$ cat state) and 0.64 ($\alpha = 2$ cat state).

measurement operator represents the measurement as if it occurred at the center of each bin.

In Fig 1, each set of points corresponds to a different data set. Our goal was to check that different data sets would have similar behavior as we change the bin size. As we can see in this figure, the highest values of fidelity corresponds to the case where we do not use discretization, as expected. We also see that smaller bin widths result in the highest fidelities. However, even the largest bin widths tested result in a fidelity loss of only 0.005 compared to the raw data.

The next set of results is presented in Fig. 2, where we show average fidelities as a function of the bin width for cat states with amplitudes $\alpha = 1$ and $\alpha = 2$. The states are reconstructed in a $M = 15$ photons Hilbert space. The fidelity for a $\alpha = 1$ cat state is always greater than the fidelity for a $\alpha = 2$ cat state, including the case when we do not use discretization. This is expected, because a $\alpha = 2$ state requires more parameters to effectively describe its density matrix in the photon number basis, so for a given amount of data, there is greater statistical uncertainty.

The fidelity for the $\alpha = 2$ cat state decreases faster than the fidelity for the $\alpha = 1$ cat state as the bin size increases. This is also expected because the $\alpha = 2$ state has more wiggles in its probability distribution, so more information is lost when the bins are larger. The average bin width used by Scott's method is 0.35 for the $\alpha = 1$ cat state, and 0.64 for the $\alpha = 2$ cat state, which results in significant fidelity loss. The Leonhardt's width indicated in Fig. 2 is obtained by using $M = 15$, the number of photons at which the Hilbert space is truncated, in Eq. (8).

Until now, as mentioned before, every measurement outcome in a given bin has been associated with the measurement operator for the quadrature value at the center of that bin. Although this may be a useful approximation for very small bins, to improve our analysis, we now change each bin's measurement operator so that it represents a measurement that occurs anywhere in the bin. For that, we numerically integrate the measurement operators over the width of each histogram bin. We identify each case by adding [POVM-center] and [POVM-integral] to the legends in the graphs.

We also add to our analysis the use of the mean photon number estimate in Leonhardt's formula, and we calculate the fidelity between ρ_{true} and the state $\rho_{\mathrm{Leonhardt}}$ estimated using the resulting bin width. Recall that Leonhardt recommends that the bin width should be equal or smaller to the one calculated using the maximum photon number in Eq. (8) but here we use the mean photon number instead.

Figs. 3 and 4 show average fidelities as functions of the bin width for cat states with amplitudes $\alpha = 1$ and $\alpha = 2$, respectively. We used a $M = 10$ photon Hilbert space to reconstruct the $\alpha = 1$ cat state, while the $\alpha = 2$ cat state was reconstructed in a $M = 15$ photon space. Fig. 5 shows the average fidelity as a function of the bin width for a squeezed vacuum state whose squeezed quadrature has a variance 3/4 of the vacuum variance, with a Hilbert space truncated at $M = 10$ photons.

For the $\alpha = 1$ cat state in Fig. 3, the estimated mean number of photons is $\overline{\langle \hat{n} \rangle} = 0.6109$ (wheras the true mean number of photons is 0.6093), which gives us, by Leonhardt's formula a bin width of 1.05. For the $\alpha = 2$ cat state in Fig. 4, the estimated mean number of photons is $\overline{\langle \hat{n} \rangle} = 3.1983$ (wheras the true mean number of photons is 3.1978), giving a bin width of 0.58. The squeezed vacuum state of Fig. 5 has an estimated mean number of photons of $\overline{\langle \hat{n} \rangle} = 0.0162$ (wheras the true mean number of photons is 0.0167), giving a bin width, by Eq. (8), of 1.54.

Analyzing the graphs shown in Figs. 3-5, we see that

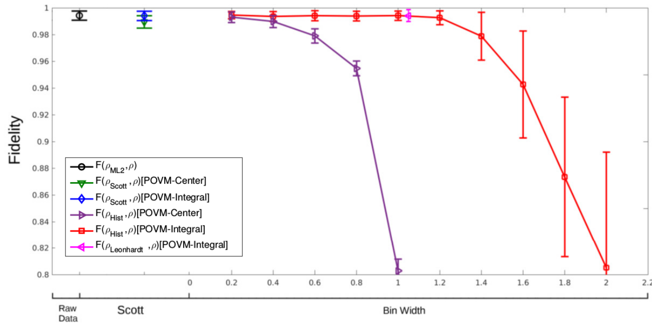

FIG. 3. Average fidelity as a function of the bin width for a cat state with amplitude $\alpha = 1$. The Hilbert space is truncated at $M = 10$ photons. The estimated mean number of photons is $\langle \hat{n} \rangle = 0.6109$, giving a bin width by Leonhardt's formula of 1.05. The mean bin width for Scott's method is 0.35.

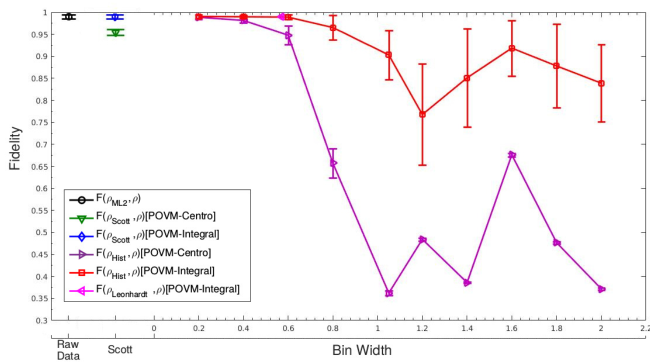

FIG. 4. Average fidelity as a function of the bin width for a cat state with amplitude $\alpha = 2$. The Hilbert space is truncated at $M = 15$ photons. The estimated mean number of photons is $\langle \hat{n} \rangle = 3.1983$, giving a bin width by Leonhardt's formula of 0.58. The mean bin width for Scott's method is 0.64.

integrating the measurement operators over the width of each histogram bin improves considerably the fidelity for all the cases. We can also see that, for this case, Leonhardt's suggestion using the estimated mean photon number can be safely used as the upper bound for the bin width. The two methods considered here, Leonhardt's and Scott's methods, give faster fidelity estimates, as we can see in Figs. 6 and 7, with no significant loss of information.

VI. CONCLUSION

We have used idealized numerical experiments to generate simulated data, performed maximum likelihood tomography on data sampled from cat states and squeezed vacuum states with and without discretization, and estimated the fidelities between the reconstructed states and the true state. We used two different methods to choose the bin width: Scott's and Leonhardt's methods. We studied using measurement operators calculated us-

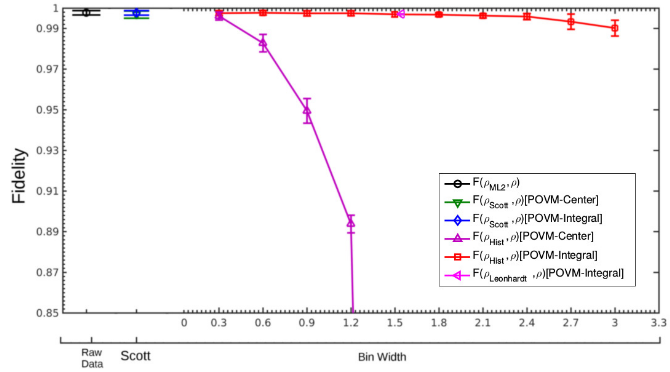

FIG. 5. Average fidelity as a function of the bin width for a squeezed vacuum state whose squeezed quadrature has a variance 3/4 of the vacuum variance. The Hilbert space is truncated at $M = 10$ photons. The estimated mean number of photons is $\langle \hat{n} \rangle = 0.0162$, giving a bin width by Leonhardt's formula of 1.54. The mean bin width for Scott's method is 0.25.

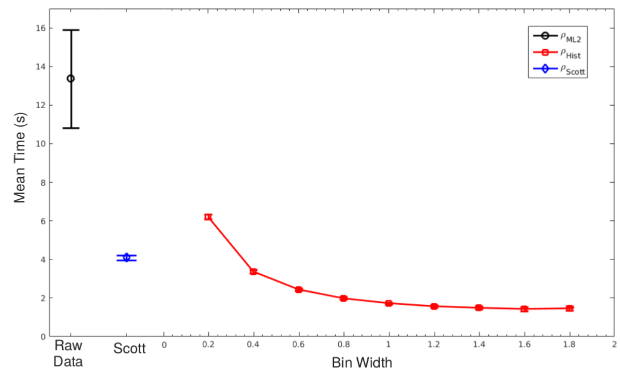

FIG. 6. Mean time as a function of the bin width for a cat state with amplitude $\alpha = 1$. The Hilbert space is truncated at $M = 10$ photons. The mean bin width for Scott's method is 0.35, and the bin width given by Leonhardt's formula is 1.05.

ing the quadrature exactly at the center of each bin and integrating the measurement operators along the length of the bin.

Scott's method calculates an optimal bin width, for each phase, based on the size and the standard deviation of the sample. Leonhardt's method recommends a bin width narrower than $q_n/2$, where q_n depends on the number of photons in the state being reconstructed. Since, in a real experiment, we do not know the mean number of photons in the state considered, we estimate the mean photon number from the quadrature measurement results.

We have found that our proposed method to find the mean number of photons from the quadrature measurement results gives accurate results. We checked that by comparing the estimated mean number of photons with the true mean number of photons for the cat states and

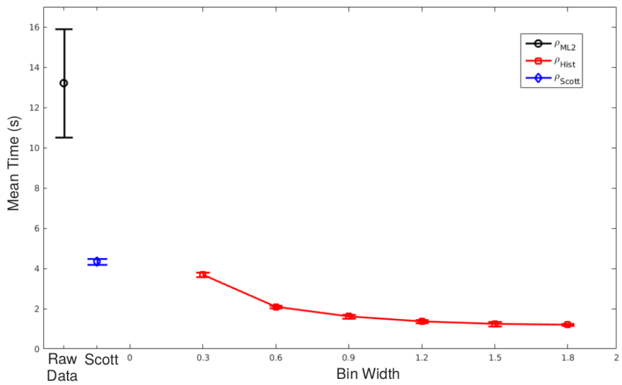

FIG. 7. Mean time as a function of the bin width for a squeezed vacuum state whose squeezed quadrature has a variance 3/4 of the vacuum variance. The Hilbert space is truncated at $M = 10$ photons. The mean bin width for Scott's method is 0.25, and the bin width given by Leonhardt's formula is 1.54.

squeezed vacuum states. We also have found that integrating the measurement operators over the width of each histogram bin significantly improves the fidelity. Using this strategy, Leonhardt's formula safely establishes an upper bound to the bin width, and both methods provides a faster statistical estimation without losing too much information. [SG: Do we have any cases in which Scott's method is really bad?]

ACKNOWLEDGMENTS

We thank ???????????? for helpful comments on the manuscript. H. M. Vasconcelos thanks the Schlumberger Foundation's Faculty for the Future program for financial support. J. L. E. Silva thanks Coordenação de Aperfeiçoamento de Pessoal de Nível Superior (CAPES) for financial support. This work includes contributions of the National Institute of Standards and Technology, which are not subject to U.S. copyright.

[1] A. Kandala, A. Mezzacapo, K. Temme, M. Takita, M. Brink, J. M. Chow, and J. M. Gambetta, "Hardware-efficient quantum optimizer for small molecules and quantum magnets," Nature **549**, 242–246 (2014), arXiv:arXiv:1704.05018.

[2] N. M. Linke, D. Maslov, M. Roetteler, S. Debnath, C. Figgatt, K. A. Landsman, K. Wright, and C. Monroe, "Experimental comparison of two quantum computing architectures," Proc. Natl. Acad. Sci. U. S. A. **114**, 3305–3310 (2017).

[3] T. Monz, D. Nigg, E. A. Martinez, M. F. Brandl, P. Schindler, R. Rines, S. X. Wang, I. L. Chuang, and R. Blatt, "Realization of a scalable shor algorithm," Science **351**, 1068–1070 (2017).

[4] V. S. Denchev, S. Boixo, S. V. Isakov, N. Ding, R. Babbush, V. Smelyanskiy, J. Martinis, and H. Neven, "What is the computational value of finite-range tunneling?" Phys. Rev. X **6**, 031015 (2016).

[5] K. Vogel and H. Risken, "Determination of quasiprobability distributions in terms of probability distributions for the rotated quadrature phase," Phys. Rev. A **40**, 2847–2849 (1989).

[6] D. T. Smithey, M. Beck, M. G. Raymer, and A. Faridani, "Measurement of the wigner distribution and the density matrix of a light mode using optical homodyne tomography: Application to squeezed states and the vacuum," Phys. Rev. Lett. **70**, 1244–1247 (1993).

[7] T. Dunn, I. A. Walmsley, and S. Mukamel, "Experimental determination of the quantum-mechanical state of a molecular vibrational mode using fluorescence tomography," Phys. Rev. Lett. **74**, 884–887 (1995).

[8] K. Banaszek, C. Radzewicz, K. Wodkiewicz, and J. S. Krasinski, "Direct measurement of the wigner function by photon counting," Phys. Rev. A **60**, 674–677 (1999).

[9] K. Banaszek, G. M. D'Ariano, M. G. A. Paris, and M. F. Sacchi, "Maximum-likelihood estimation of the density matrix," Phys. Rev. A **61**, 010304(R) (2000).

[10] A. G. White, D. F. V. James, W. J. Munro, and P. G. Kwiat, "Exploring hilbert space: Accurate characterization of quantum information," Phys. Rev. A **65**, 012301 (2002).

[11] A. Ourjoumtsev, H. Jeong, R. Tualle-Brouri, and P. Grangier, "Generation of optical 'schrödinger cats' from photon number states," Nature **448**, 784–786 (2007).

[12] J. S. Neergaard-Nielsen, B. Melholt Nielsen, C. Hettich, K. Mø lmer, and E. S. Polzik, "Generation of a superposition of odd photon number states for quantum information networks," Phys. Rev. Lett..

[13] I. L. Chuang and M. A. Nielsen, "Prescription for experimental determination of the dynamics of a quantum black box," J. Mod. Optics **44**, 2455–2467 (1997).

[14] J. F. Poyatos, J. I. Cirac, and P. Zoller, "omplete characterization of a quantum process: The two-bit quantum gate," Phys. Rev. Lett. **78**, 390–393 (1997).

[15] J. B. Altepeter, D. Branning, E. Jeffrey, T. C. Wei, P. G. Kwiat, R. T. Thew, J. L. OBrien, M. A. Nielsen, and A. G. White, "Ancilla-assisted quantum process tomography," Phys. Rev. Lett. **90**, 193601 (2003).

[16] G. M. D'Ariano and L. Maccone, "Measuring quantum optical hamiltonians," Phys. Rev. Lett. **80**, 5465–5468 (1998).

[17] M. A. Nielsen, E. Knill, and R. Laflamme, "Complete quantum teleportation using nuclear magnetic resonance," Nature.

[18] M. W. Mitchell, C. W. Ellenor, S. Schneider, and A. M. Steinberg, "Diagnosis, prescription and prognosis of a bell-state filter by quantum process tomography," Phys. Rev. Lett..

[19] J. L. O'Brien, G. J. Pryde, A. Gilchrist, D. F. V. James, N. K. Langford, T. C. Ralph, and A. G. White, "Quantum process tomography of a controlled-not gate," Phys.

Rev. Lett..
[20] C. Kupchak, S. Rind, B. Jordaan, and E. Figueroa, “Quantum process tomography of an optically-controlled kerr non-linearity,” Sci. Rep. **5**, 16581 (2015).
[21] A. Luis and L. L. Sanchez-Soto, “Complete characterization of arbitrary quantum measurement processes,” Phys. Rev. Lett. **83**, 3573–3576 (1999).
[22] J. Fiurasek, “Maximum-likelihood estimation of quantum measurement,” Phys. Rev. A **64**, 024102 (2001).
[23] G. M. D’Ariano, L. Maccone, and P. Lo Presti, “Quantum calibration of measurement instrumentation,” Phys. Rev. Lett. **93**, 250407 (2004).
[24] J. S. Lundeen, A. Feito, H. Coldenstrodt-Ronge, K. L. Pregnell, Ch. Silberhorn, T. C. Ralph, J. Eisert, M. B. Plenio, and I. A. Walmsley, “Tomography of quantum detectors,” Sci. Rep. **5**, 27–30 (2009).
[25] S. Lloyd and S. L. Braunstein, “Quantum computation over continuous variables,” Phys. Rev. Lett. **82**, 1784 (1999).
[26] D. Gottesman, A. Kitaev, and J. Preskill, “Encoding a qubit in an oscillator,” Phys. Rev. A **64**, 012310 (2001).
[27] S. D. Bartlett, H. de Guise, and B. C. Sanders, “Quantum encodings in spin systems and harmonic oscillators,” Phys. Rev. A **65**, 052316 (2002).
[28] H. Jeong and M. S. Kim, “Efficient quantum computation using coherent states,” Phys. Rev. A **65**, 042306 (2002).
[29] T. Ralph, A. Gilchrist, G. Milburn, W. Munro, and S. Glancy, “Quantum computation with optical coherent state,” Phys. Rev. A **68**, 042319 (2003), quant-ph/0306004.
[30] T. Ralph, “Continuous variable quantum cryptography,” Phys. Rev. A **61**, 010303(R) (1999).
[31] M. Hillery, “Quantum cryptography with squeezed states,” Phys. Rev. A **61**, 022309 (2000).
[32] Ch. Silberhorn, T. C. Ralph, N. Lü tkenhaus, and G. Leuchs, “Continuous variable quantum cryptography: Beating the 3 db loss limit,” Phys. Rev. Lett. **89**, 167901 (2002).
[33] S. Pirandola, S. Mancini, S. Lloyd, and S. L. Braunstein, “Continuous-variable quantum cryptography using two-way quantum communication,” Nature Phys. **4**, 726–730 (2008), arXiv:quant-ph/0304059.
[34] F. S. Luiz and G. Rigolin, “Teleportation-based continuous variable quantum cryptography,” **16**, 58 (2017).
[35] T. Eberle, S. Steinlechner, J. Bauchrowitz, V. Hä ndchen, H. Vahlbruch, M. Mehmet, H. Mü ller Ebhardt, , and R. Schnabel, “Quantum enhancement of the zero-area sagnac interferometer topology for gravitational wave detection,” Phys. Rev. Lett. **104**, 251102 (2004).
[36] R. Demkowicz-Dobrzaski, K. Banaszek, and R. Schnabel, “Fundamental quantum interferometry bound for the squeezed-light-enhanced gravitational wave detector geo 600,” Phys. Rev. A **88** (2013).
[37] L. Vaidman, “Teleportation of quantum states,” Phys. Rev. A **49**, 1473 (1994).
[38] S. L. Braunstein and H. J. Kimble, “Teleportation of continuous quantum variables,” Phys. Rev. Lett. **80**, 869 (1998).
[39] Q. He, L. Rosales-Zrate, G. Adesso, and M. D. Reid, “Secure continuous variable teleportation and einstein-podolsky-rosen steering,” Phys. Rev. Lett. **115**, 180502 (2015).
[40] S. L. Braunstein and H. J. Kimble, “Dense coding for continuous variables,” Phys. Rev. A **61**, 042302 (2000).
[41] J. Lee, S. Ji, J. Park, and H. Nha, “Continuous-variable dense coding via a general gaussian state: Monogamy relation,” Phys. Rev. A **90**, 022301 (2014).
[42] N. J. Cerf and S. Iblisdir, “Optimal n-to-m cloning of conjugate quantum variables,” Phys. Rev. A **62**, 040301(R) (2000).
[43] S. L. Braunstein, N. J. Cerf, S. Iblisdir, P. van Loock, and S. Massar, “Optimal cloning of coherent states with a linear amplifier and beam splitters,” Phys. Rev. Lett. **86**, 4938 (2001).
[44] A I Lvovsky, “Iterative maximum-likelihood reconstruction in quantum homodyne tomography,” J. Opt. B:Quantum Semiclass. Opt. **6**, S556 (2004), arXiv:quant-ph/0311097.
[45] D. Scott, “Scott’s rule,” WIREs Comp. Stat. **2**, 497–502 (2010).
[46] U. Leonhardt, M. Munroe, T. Kiss, Th. Richter, and M.G. Raymer, “Sampling of photon statistics and density matrix using homodyne detection,” Opt. Commun. **127**, 144–160 (1996).
[47] Jaroslav Řeháček, Zdeněk Hradil, E. Knill, and A. I. Lvovsky, “Diluted maximum-likelihood algorithm for quantum tomography,” Phys. Rev. A **75**, 042108 (2007), arXiv:quant-ph/0611244v2.
[48] S. C. Glancy, E. Knill, and M. Girard, “Gradient-based stopping rules for maximum-likelihood quantum-state tomography,” New J. Phys. **14**, 095017 (2012), arXiv:1205.4043 [quant-ph].
[49] William J. Kennedy Jr. and James E. Gentle, Statistical Computing (Marcel Dekker, Inc., New York, 1980) see section 6.4.3.
[50] U. Leonhardt, Measuring the Quantum State of Light (Cambridge University Press, New York, 1997).
[51] M. G. Raymer and M. Beck, “Experimental quantum state tomography of optical fields and ultrafast statistical sampling,” in Quantum State Estimation, Vol. 649, edited by M. G. A. Paris and J. Řehček (Springer, 2004) Chap. 7, p. 259, http://muj.optol.cz/hradil/PUBLIKACE/2004/teorie.pdf.
[52] M. Munroe, Ultrafast photon statistics of cavityless laser light, Ph.D. thesis, University of Oregon (1996).